Energy transport in aluminum targets irradiated by a 263-nm laser

A. Yamauchi, K. A. Tanaka, R. Kodama, M. Kado, T. Yamanaka, T. Mochizuki,[a)]
S. Nakai, and C. Yamanaka[b)]
Institute of Laser Engineering, Osaka University, Yamada-oka 2-6, Suita, Osaka 565, Japan

(Received 9 November 1987; accepted for publication 5 January 1988)

Emission from the rear side of 263-nm laser irradiated thin foil targets shows the temporal profile of rear surface heating by several processes with different energy transport mechanisms. Formation and decay of shock waves are observed by varying target thickness. Propagation of a thermal conduction wave is clearly separated from the shock propagation.

The study of energy transport is of particular importance to laser fusion. The preheat should be minimal ($\leqslant 1\%$), and the absorbed energy rate and following compression must be as high as possible. Energy transport may affect directly the level of preheat and the degree of compression. There are several target heating processes, such as those due to thermal conduction, shock waves, x-ray radiation and hot electron.[1] A short wavelength laser ($\lambda \leqslant 1\,\mu$m) is known to be advantageous for laser fusion because of its high-energy absorption and low hot-electron generation.[2] We observed rear side emission[3–5] of thin foil targets irradiated by a 263-nm laser. By using this method[5] not only shock wave propagation but also radiation heating and the thermal conduction wave could be observed.

In this letter the growth and decay of shock waves are observed and are compared with a model of the shock formation. Also observed is the emission due to thermal conduction. We then discuss the processes of the energy transport. One arm of the Gekko IV four beam glass laser system (ω_0: $\lambda = 1.053\,\mu$m) was quadrupled ($4\omega_0$: $\lambda = 0.263\,\mu$m) with the use of two KDP (potassium dihydrogen phosphate) crystals. The $4\omega_0$ energy was around 1 J with a 400-ps pulse full width at half-maximum. Using a quartz lens whose focal length was 80 cm, a typical spot size was 100 μm in diameter which contains 90% of the laser energy at 0° of incident angle. On target intensity was a few times 10^{13} W/cm^2. Thin aluminum foils were used for targets whose thickness ranged from 0.7 to 20 μm. Irradiating the front side of the target, the absorbed laser energy is transported through the target via several mechanisms, causing rear side emissions. Emissions from the rear side were optically relayed onto a time streak camera (S-20) slit by quartz lenses at an observation angle of 45° to the target normal. The time resolution was 30 ps. A time fiducial was introduced into the streak camera by an optical fiber which picked up a part of the incoming laser light. Using a tungsten lamp, the absolute sensitivity of this streak camera was calibrated *in situ* so that a blackbody temperature could be assigned for the rear side emission.

Temporally resolved emissions from the rear side of the alminum foils are shown in Figs. 1(a)–1(e). These data show absolute temperatures in the vertical axis, which were obtained numerically with the assumption of blackbody ra-

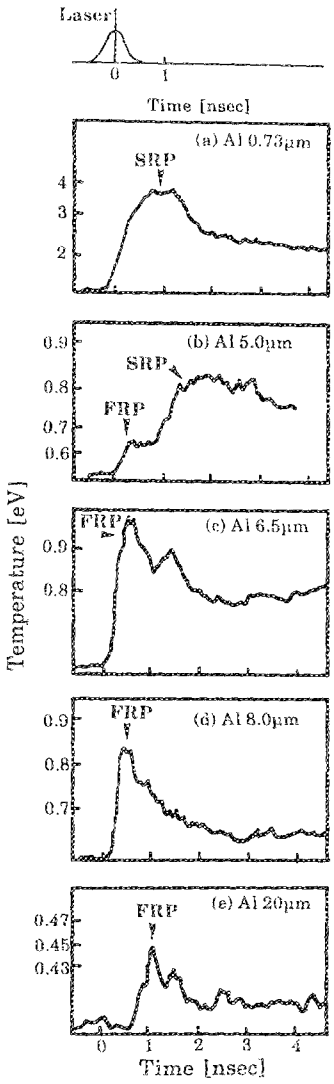

FIG. 1. Rear side emissions of aluminum foil targets: (a) 0.73 μm, (b) 5.0 μm, (c) 6.5 μm, (d) 8.0 μm, (e) 20 μm. The temperature (vertical axis) was calculated from fitting to a blackbody emission. Calibration was performed with a tungsten lamp. FRP means fast rise peak. SRP means slow rise peak.

[a)] Present address: R&D center, HOYA, Musashino 3-3-1, Akishima, Tokyo 196, Japan.

[b)] Present address: Institute for Laser Technology, Yamada-oka 2-6, Suita, Osaka 565, Japan.

 0003-6951/88/100786-03$01.00

diation, and comparing to the calibrated tungsten lamp measurement. The time is shown in the horizontal axis. The time zero is the laser peak which was obtained absolutely by the optical fiber fiducial. In Fig. 1 (a), the emission shows a SRP (slow rise peak: $\Delta T_{\text{rise}} \sim 1$ ns) and its peak temperature corresponds to 3.8 eV. After the peak the emission decays slowly. And it was also confirmed by a slow sweep streak camera that no more peaks appear after the SRP. The emission history shows a change for targets thicker than 5 μm. The SRP delays and decays, and a FRP (fast rise peak: $\Delta T_{\text{rise}} = 100$–200 ps) appears in front of the SRP. For a 6.5-μm-thick target the FRP grows and the SRP decays further. For a target thicker than 8.0 μm [Figs. 1(d) and 1(e)], only the FRP could be observed within the time frame of the streak camera, and the SRP came much later in time, and the FRP also decayed with target thickness. Separation between the FRP and SRP was 7 ns, for example, for the 7 μm target. In Fig. 2 (a) the temperature of the observed FRP and SRP is plotted as a function of the thickness. The thicker the targets, the lower the SRP temperatures become. The FRP temperature rises till 7 μm thickness and then the FRP temperature decays. From both figures the FRP and SRP appear to be caused by different processes.

Absorbed energies may be transported from the front side of the target to the rear by several possible processes: direct heating by transmitted x rays, shock wave propagation, and thermal conduction. Heating by suprathermal electrons, which usually results from nonlinear coupling of laser and plasmas, is excluded since the collisional absorption process is so dominant in $4\omega_0$ laser plasmas.[2]

First we consider the heating by x rays. When a target is irradiated by the 4ω laser, the absorbed laser energy is converted to the x-ray energy with a relatively high conversion efficiency.[6] And a part of this x-ray energy is transported through the target, and is reabsorbed at the rear side of the target (direct heating). The distribution of the x-ray deposited energy may be determined by the absorption cross section. The absorption distribution and the deposited energy is expressed as[7]

$$T_X(x_0) = \left.\frac{dT}{dx}\right|_{x_0} \Delta x = \frac{-2}{3kNx_0^2}\int (1 + N\sigma x_0)e^{-N\sigma x} E_f(h\nu)\,d h\nu, \quad (1)$$

where E_f $(h\nu)$ is the experimental x-ray emission spectrum, k is the Boltzmann constant, N is the density of the target, σ is the absorption cross section, x_0 is the depth of the target, and $T_X(x_0)$ is the deposited energy at the depth $x = x_0$ of the heated target. From this calculation the rear side could be heated by direct x-ray heating up to a temperature as shown in Table I which is too low compared to the observed rear side temperatures. Thus the observed rear side emission is not caused by x-ray heating.

Next we consider the thermal conduction including the ablation process. According to the rocket model the ablation speed is expressed as[3,8]

$$\frac{d}{dt} d_a\,[\text{cm/s}] = 110\times 10^3 \left(\frac{\Phi_a\,[\text{W/cm}^2]}{10^{14}}\right)^{1/3} \lambda\,[\mu\text{m}]^{-4/3} \times \frac{1}{\rho_0[\text{g/cm}^3]} = 10^5\ \text{cm/s}. \quad (2)$$

From this equation the quasi-burnthrough time τ_B can be estimated. These burnthrough times agree with the SRP's shown in Fig. 1; 0.73 μm aluminum is about 0.7 ns, for example. So the SRP emissions could well be caused by the thermal conduction driven by the ablation. And in a target thicker than 5 μm the SRP velocity slows down, since the front of thermal conduction loses its driving energy after the laser pulse. Thus the SRP's observed for the target thickness less than 5 μm are consistent with the emissions caused by the ablation and thermal conduction.

Out of these possible mechanisms of energy transport in solid foils, the x-ray heating and the mass ablation have been discussed so far. The rest of this section is devoted to show the FRP's are due to the shock heating. We first estimate the shock amplitude and the arrival time in the Al target. The shock wave front grows and decays when it propagates. Assuming the incident temporal shape of pressure is a triangular pulse, the shock front grows because the shock velocity increases with its shock amplitude. The shock decay is expressed as[9]

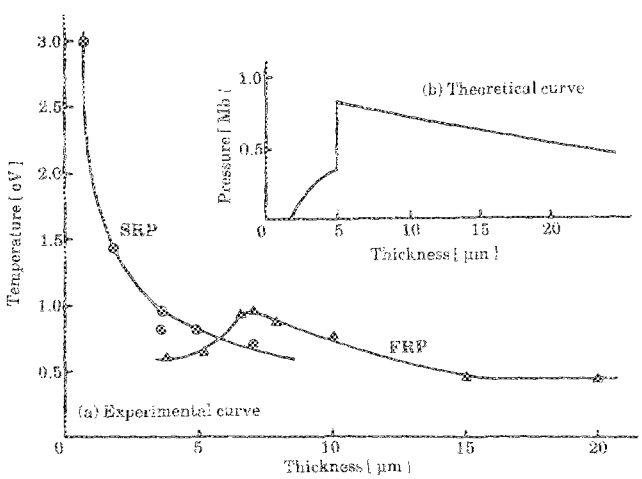

FIG. 2. (a) Temperature vs target thickness for SRP and FRP. There are two types of peak: a slow rise peak (SRP) and a fast rise peak (FRP). The FRP has a peak temperature at the thickness of 7 μm Al. The intensity of the SRP decreases monotonically with target thickness. (b) Calculated pressure profile. We assume that a triangle temporal shape pressure is introduced for this calculation. The value of the pressure is 1 Mb. The temporal width is 400 ps at the half-maximum. The shock wave grows over some distance and reaches maximum pressure at the depth of 5 μm and then decays.

TABLE I. X-ray deposited energy in the aluminum target is calculated using the experimental x-ray emission data and absorption cross section.

Target thickness x_0 (μm)	Deposited energy T_x (eV)
0.73	1.60
5.0	5.0×10^{-3}
6.5	1.8×10^{-3}
8.0	7.7×10^{-4}
20	9.9×10^{-6}

$$\frac{DP}{Dt} = -A\frac{\partial P}{\partial t} = A\left[\frac{\tau_p}{P_m} + \frac{x_i}{(C+u)^2_{P_i}}\left(\frac{du}{dP} + \frac{dC}{dP}\right)\right]^{-1}, \quad (3)$$

where P is the pressure, A is the coefficient for the material, τ_p is the incident laser pulse duration, P_m is the maximum pressure, C is the sound velocity, and u is the particle velocity. Figure 2 (b) shows a calculated curve of the shock front pressure in an aluminum target using Eq. (3). This shock wave calculation gives us a profile of the shock front formation and decay. The shock front grows with the target thickness and reaches its maximum value of several Mb at 7 μm, and then decays for the target thicker than that. From the Hugoniot relation in a target the higher the shock amplitude is, the faster the shock velocity is. Thus the amplitude of the shock front increases with shock penetration. From our data the shock front reaches its peak value at about 7 μm depth. For a thickness more than 7 μm the shock starts decaying, since the rarefaction wave is usually much faster than the speed of the shock and catches the shock front.[10] Experimental points are plotted as dots (▲) in Fig. 2 (a) and show a good agreement with the theoretical curve. At the decaying part, the model shows more gradual decay because a pure one dimensionality is assumed, while a more three-dimensional plasma expansion accelerates the rarefaction wave in the experiment.

In conclusion, we have observed the formation and the decay of a 4ω laser induced shock wave in the aluminum foil targets. The shock wave (FRP) had a peak value at the depth of 7 μm in the Al foil targets at the irradiation intensity of a few times 10^{13} W/cm^2. Also observed were the temporally resolved emissions due to the transmission of the thermal conduction (SRP) in Al foil targets which was distinctively separated from the shock front.

The authors greatly acknowledge invaluable comments by Dr. T. Yabe. They also thank N. Doi and H. Nakano for their technical assistance and the Target group for the target fabrication.

[1]S. P. Obenschain, R. R. Whitlock, E. A. McLean, and B. H. Ripin, Phys. Rev. Lett. **50**, 44 (1983); S. H. Gold, and E. A McLean, J. Appl. Phys. **53**, 784 (1982).
[2]A. G. M. Maaswinkel, K. Eidmann, and R. Sigel, Phys. Rev. Lett. **42**, 1625 (1979); W. Seka, R. S. Craxton, J. Delettrez, L. Goldman, R. Keck, R. L. McCrory, D. Shvarts, J. M. Soures, and R. Boni, Opt. Commun. **40**, 437 (1982); W. C. Mead, E. M. Campbell, K. G. Estabrook, R. E. Turner, W. L. Kruer, P. H. Y. Lee, B. Pruett,V. C. Rupert, K. G. Tirsell, G. L. Stradling, F. Ze, C. E. Max, and M. D. Rosen, Phys. Rev. Lett. **47**, 1289 (1981).
[3]R. Fabbro, B. Faral, F. Cottet, and J. P. Romain, J. Appl. Phys. **56**, 3204 (1984).
[4]E. A. McLean, S. H. Gold, J. A. Stamper, R. R. Whitlock, H. R. Griem, S. P. Obenschain, B. H. Ripin, S. E. Bodner, and M. J. Herbst, Phys. Rev. Lett. **45**, 1246 (1980); A. Ng, D. Parfeniuk, L. Da Silva, and F. Celliers, Laser Part. Beams **4**, 555 (1986); F. Cottet, J. P. Romain, R. Fabbro, and B. Faral, Phys. Rev. Lett. **52**, 1884 (1984); A. Ng, D. Parfeniuk, and L. DaSilva, Opt. Commun. **53**, 389 (1985).
[5]A. Ng, D. Parfeniuk, L. DaSilva, and D. Pasini, Phys. Fluids **28**, 2915 (1985).
[6]R. Kodama, K. Okada, N. Ikeda, M. Mineo, K. A. Tanaka, T. Mochizuki, and C. Yamanaka, J. Appl. Phys. **59**, 3050 (1986).
[7]M. H. Key, in *Energy Transport in Laser Produced Plasmas* (*Radiation in Plasmas*), edited by McNamara (World Scientific, Singapore, 1984), Vol. I, p. 478.
[8]R. Fabbro, E. Fabre, F. Amiranoff, C. Garban-Labaune, J. Virmont, M. Weinfeld, and C. E. Max, Phys. Rev. A **26**, 2289 (1982).
[9]F. Cottet and J. P. Romain, Phys. Rev. A **25**, 576 (1982).
[10]Ya. B. Zel'dovich and Yu. P. Raizer, *Physics of Shock Waves and High-Temperature Hydrodynamic Phenomena* (Academic, New York, 1966).